

# Mechanism of Formation of Plane Surfaces with an Electric Arc

V. M. Bokov<sup>a,\*</sup>, O. F. Sisa<sup>a,\*\*</sup>, and V. Ya. Mirzak<sup>a</sup>

<sup>a</sup>Central Ukrainian National Technical University, Kropivnitskii, 25006 Ukraine

\*e-mail: victor.alia.knty@gmail.com

\*\*e-mail: sisaoleh@ukr.net

Received March 12, 2018; revised April 18, 2018; accepted May 18, 2018

**Abstract**—A new method is presented for two similar plane surfaces of high-performance dimensional treatment with an electric arc (DTEA) where the components are hard-to-cut materials in a bipolar mode without the traditional application of an electrode tool. In comparison to DTEA with the use of an electrode tool, this new method provides an increase in the efficiency of treatment by 230%. It is shown that for passing from unipolar DTEA of VK-15 hard alloy with a graphite electrode-tool to bipolar DTEA of two samples of the same alloy, a considerable increase in heat energy of the cathode area is found due to the energy of the arc column, which can overrun the heat energy of the anode area and lead to inversion, that is, a change in the direction of the prevailing electric erosion. This increase in the heat energy of the arc cathode area explains the growth in the productivity of the bipolar DTEA of two samples of the hard alloy VK-15 over the unipolar one.

**Keywords:** electric arc, hydrodynamic flow, bipolar mode, hard alloy

**DOI:** 10.3103/S1068375519020066

## INTRODUCTION

As hard-to-cut materials are produced in larger and large numbers due to the introduction of modern technological processes into the machine-building industry [1–3], there is often the need for a quick removal of a big stock before subsequent finish machining. Such parts include punches, matrices, rolling instrument (rolls) of hardened steels and alloys, and hard alloys. Electroerosion machining methods are usually used to remove this stock [4–5] by applying non-steady forms of electric discharge (electric sparks or electric pulses) to break the electrode workpiece (EW). The machining comes with pauses, leading to poor productivity.

The rate of processing depends on how quick heat energy is introduced into the treatment zone [6–8] (according to the level of the current). On the other hand, the stability of the process, other conditions being equal, is determined by the balance between the quantities of the cut metal and the metal removed from the interelectrode gap (erosion products). It is clear that the highest rate of electroerosion processing is achieved when heat energy is continuously introduced into the treatment zone, i.e., without pause (when the pulse ratio is  $q = 1$ ). Here, the electric arc is an instrument.

Works [9–11] describe the method of the dimensional treatment of metals with an electric arc (DTEA). In this process, a tenfold or larger increase in productivity over electric pulse machining can be guaranteed, due to the continuity of the arc burning

through time and the possibility of using a stronger current. The DTEA process is usually performed using a graphite electrode tool (ET). An electric arc in the cross hydrodynamic flow of working fluid is struck between EW and ET. This means that some part of the energy delivered into the treatment zone is spent not for production but to break the ET.

The authors consider that the performance of plane surface treatment can be greatly increased using the energy noted above to break the EW.

This paper is dedicated to the investigation of new methods of effective electric arc processing [12] when an electric arc is struck between similar plane surfaces of two EWs, i.e., without the traditional application of an ET.

## PROCEDURE

Comparative analysis is used to substantiate the new process scheme of plane surface formation. DTEA methods for a plane surface with the use or not of an ET were the comparison objects (Table 1).

Thus, with the known method of DTEA of a plane surface, in the unipolar mode, the electric arc burns in the hydrodynamic flow of a working fluid between a graphite ET and an EW. As a result, the following is observed: a comparatively low performance of the process, as a part of energy is spent in the breakage of the graphite ET; a considerable flatness appears due to the increase in the frontal spark gap (FSG) towards the evacuation of erosion products of mainly EW; a higher

**Table 1.** Comparative analysis of process schemes of plane surface formation with or without use of an electrode tool and velocity profiles in the frontal spark gap

Treatment phase	Known method of DTEA of plain surface: "graphite ET–VK-15 alloy" electrode pair, unipolar mode (series 1)	New method of DTEA of plain surface: "VK-15 alloy–VK-15 alloy" electrode pair, bipolar mode (series 2)
Initial		
Intermediate		

(1) graphite ET, (2) VK-15 alloy, (3) arc, (4) erosion products, (5) hydrodynamic flow.

resistance to fluid flow due to ET wear with higher electric energy demand to develop a necessary hydrodynamic flow mode in the arcing area. In the proposed DTEA method of a plane surface, a new process scheme of formation is used when two EWs are processed simultaneously: an electric arc in hydrodynamic fluid flow is struck between their similar plane surfaces. However, in contrast with known methods, treatment polarity is periodically changed to make the removal of metal uniform from both the EWs. This mode is further called bipolar. The new scheme of formation has a number of advantages. First, it aids higher treatment performance, due to a more complete usage of electric energy and simultaneous processing of two parts. Second, it provides almost half the flatness, in comparison with the existing scheme, due to the peculiarities of its formation: the growth in the FSG at the outflow is uniform, at the cost of both upper and lower EWs. Third, it also makes it possible to control the uniformity of the distribution of the flow rate in the radial axis of the FSG, thus ensuring an equal quality of plane surface treatment. Fourth, it insures a lower production cost of the DTEA of plane surfaces, as it is not necessary to manufacture and use relatively expensive graphite ETs. Finally, it allows the production electrode erosion products to be produced, free from foreign matters, as a valuable product for further application.

The physical and process characteristics of the two DTEA methods for plane surfaces are simulated using the PRIAM software package.

Simulation objects include such process characteristics as processing performance  $M$ ,  $\text{mm}^3/\text{min}$ ; specific processing performance  $M_a$ ,  $\text{mm}^3/\text{A min}$ ; specific energy consumption  $a$ ,  $\text{kWh/kg}$ ; lateral external FSG  $\delta$ ,  $\text{mm}$ ; relative linear wear of ET  $\gamma$ ,  $\%$ ; roughness of the process surface  $Ra$ ,  $\mu\text{m}$ ; and relative non-uniformity of processing  $\Delta$ ,  $\%$ . In addition, simulation objects had such physical parameters of the arc under the conditions of the DTEA bipolar mode as current density in the arc  $j$ ,  $\text{A}/\text{mm}^2$ ; electric field intensity in the arc column  $E$ ,  $\text{V}/\text{mm}$ ; and spatial density of heat power in the arc column  $K$ ,  $\text{kW}/\text{mm}^3$ .

Strength  $I$  of the process current, the frequency of change in its polarity  $f$ , static pressure of the working fluid  $P_{st}$  at the flow inlet into FSG, processing area  $F$ , and processing depth  $h$  were used as factors.

MPG-7 graphite was used to produce ET, and VK-15 hard alloy was used as EW.

The experimental investigations were carried out using a Duga 8G electroerosion machine. The oscillographic testing of the strength of unipolar and bipolar current, the voltage on the electrodes, and the static pressure of the working fluid at the flow inlet into the FSG were presented with the help of a ATsP L-264 card with a conversion frequency of 200 kHz, and the software package Oscilloskop. The hydraulic fluid consumption was measured with the help of a flow rate meter with a no-contact counter of infrared radial signals in a nonvisible spectrum, in a wavelength of  $\lambda = 1.12 \mu\text{m}$ . An MIM-8 metallographic microscope and an REM-106I scanning electron microscope were

**Table 2.** Mathematical models of DTEA process characteristics

Mathematical model	Scaling relation of factors
Unipolar mode, electrode pair “graphite ET–hard alloy”	
$M = 1018 + 772x_1 - 108x_3 - 85x_2 - 72x_1x_3 - 60x_1x_2$	$x_1 = 0.00667(X_1 - 250)$ $x_2 = 5(X_2 - 1)$ $x_3 = 0.00623(X_3 - 560.5)$ $x_4 = 0.667(X_4 - 2.5)$
$M_a = 3.52 + 0.982x_1 - 0.403x_3 - 0.311x_2 + 0.11x_2x_3 - 0.097x_4$	
$a = 10.36 - 2.47x_1 + 2.17x_3 - 1.4x_1x_3 + 1.19x_4 - 1.06x_1x_4 + 0.76x_2x_4 - 0.70x_3x_4 + 0.65x_2x_3 + 0.41x_1x_2$	
$Ra = 40.8 + 19.1x_1$	
$\delta_s = 0.0712 + 0.0162x_3 - 0.0075x_2$	
$\gamma_1 = 5.26 + 2.48x_2 + 1.54x_3 + 0.955x_2x_3 - 0.735x_4$	
where: $X_1 \rightarrow I, A$ ; $X_2 \rightarrow P_{st}, MPa$ ; $X_3 \rightarrow F, mm^2$ ; $X_4 \rightarrow h, mm$	
Bipolar mode, electrode pair “hard alloy–hard alloy”	
$M = 1051 + 312x_1 - 115x_3 - 76x_1x_3 - 56x_2$	$x_1 = 0.02(X_1 - 150)$ $x_2 = 5(X_2 - 1)$ $x_3 = 0.00623(X_3 - 560.5)$ $x_4 = 4.44(X_4 - 0.275)$
$M_a = 7.09 - 0.672x_3 - 0.38x_2 - 0.284x_1 - 0.281x_1x_3 - 0.186x_4$	
$a = 4.41 + 0.441x_3 + 0.226x_1 + 0.223x_2 + 0.213x_1x_3 + 0.126x_4$	
$Ra = 17.5 - 3.50x_2 + 1.25x_3 + 0.50x_1 - 0.25x_2x_3$	
$\Delta = 1.46 - 0.93x_4 - 0.309x_3 + 0.127x_1$	
where: $X_1 \rightarrow I, A$ ; $X_2 \rightarrow P_{st}, MPa$ ; $X_3 \rightarrow F, mm^2$ ; $X_4 \rightarrow f, Hz$	

used for the metallographic study of the VK-15 hard alloy.

## EXPERIMENTAL

With the aim of relating the electric and hydraulic modes of processing, the geometric parameters of the electrodes, and the possibility of controlling the performance and accuracy of treatment and the quality of the processed surface, as well as forecasting these parameters, mathematical models of the process characteristics of the DTEA of plane surfaces of the VK-15 hard alloy samples were created (Table 2).

These mathematical models helped calculate the relationships between the performance  $M$  of processing the plane surfaces with DTEA, using and not using an electrode tool and current strength  $I$  and comparing them in the same initial conditions: current strength range  $I = 100\text{--}200$  A; processing area  $F = 400$  mm<sup>2</sup>; and  $P_{st} = 0.8$  MPa (Fig. 1). A comparative analysis of the physical parameters of the electric arc and the process characteristics has been performed to explain the physical regularities of the bipolar mode of the DTEA of plane surfaces (Table 3).

In the course of the DTEA of plane surfaces without the use of ET, no lateral FSG is formed, and it is difficult to measure the terminal FSG. Without knowledge of the value of the terminal FSG, it is impossible to control the flow rate at the inlet into the

terminal FSG. The flow rate depends on the value of the terminal FSG and the consumption of hydraulic fluid. The control of static pressure of the working fluid at the flow inlet into the terminal FSG and fluid consumption ensures the necessary terminal FSG, and consequently, the necessary flow rate at the inlet into it. With this aim, an analytic dependence (1) is obtained for static pressure  $P_{st}$  of the organic working fluid in the tight machine chamber with regard to a group of factors that characterize the geometric parameters of the interelectrode gap (IEG) ( $\delta_{t(in)}, D$ ),

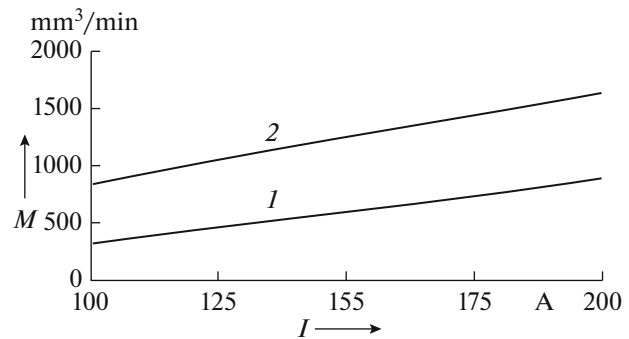


**Fig. 1.** Performance  $M$  of processing of plane surfaces using DTEA methods versus current strength  $I$ : (1) unipolar mode, graphite–hard alloy electrode pair; (2) bipolar mode, hard alloy–hard alloy electrode pair.

**Table 3.** Comparative analysis of physical parameters of electric arc and process characteristics under the conditions of the DTEA unipolar and bipolar modes

Treatment mode	Treatment scheme and distribution of electric field in arc	$P$ , W	$U_{a+c}$ , V	$U_{cl}$ , V	$M$ , mm <sup>3</sup> /min	$a$ , kW h/kg	$\delta = \delta_1$ , mm
Unipolar		3000	16	14	1020	6.24	0.10
Unipolar		3000	19	11	351	9.99	0.05
Bipolar		3000	23	7	800	3.84	0.03

$I = 100 \text{ A} = \text{const}$ ;  $U = 30 \text{ V} = \text{const}$ ;  $P_{st} = 0.8 \text{ MPa} = \text{const}$ .

quantitative and qualitative parameters of the fluid ( $Q$ ,  $\rho$ ,  $v$ ), and hydraulic resistance in different sections of

IEG ( $\xi_{in}$ ,  $\xi_p$ ), and development of the nomograph (Fig. 2):

$$P_{st} = \frac{\rho Q}{\pi D \delta_{t(in)}^2} \left\{ \frac{Q}{2\pi D} (\xi_{in} + 0.25\xi_{out}) + \frac{48v}{D^2 \delta_{t(in)}} a \right.$$

$$\left. = \int_{\sqrt{2D\delta_{t(in)}}}^{b=0.5D} (r_i - \sqrt{2D\delta_{t(in)}}) \left( 0.5 + \frac{r_i - \sqrt{2D\delta_{t(in)}}}{D - 2\sqrt{2D\delta_{t(in)}}} \right)^3 r_i dr \right\}. \tag{1}$$

The physical mechanism of electric erosion in the bipolar mode of DTEA of two hard alloy electrodes is closely associated with the quality of the heat sources on the electrodes, the polarity, and the dynamics of the process.

The quality of heat sources for the electrodes is characterized by the spatial density of the heat power in the cathode and the heat sources for the anode. In, the spatial density of the heat power in the cathode and anode heat sources is determined by current density and electric field intensity, respectively, in those regions of the arc. Under the conditions of the bipolar mode of the simultaneous DTEA of two samples of the VK-15 hard alloy, mathematical models (Table 4) are created to study the influence of variable factors (Fig. 3) on the average current density in the arc  $j_i$ , the

electric field intensity in the arc column  $E$ , and the spatial density of heat power in arc column  $K$ .

To investigate the dynamics of the process and the physical mechanism of the bipolar DTEA, there fractographies of the terminal surface of the VK-15 hard alloy sample are performed following after bipolar DTEA (Fig. 4); fractographies of the single cathode and anode arc tracings on the previously ground surfaces of the electrode pair VK-15 alloy–VK-15 alloy (Fig. 5); oscillograms of current strength  $I$ , voltage on the electrodes  $U$ , and static pressure of the working fluid are performed at the inlet into FSG  $P_{st}$  (Fig. 6); and the energy balance of the bipolar electric arc under the conditions of DTEA of the hard alloy electric pair is established (Fig. 7).

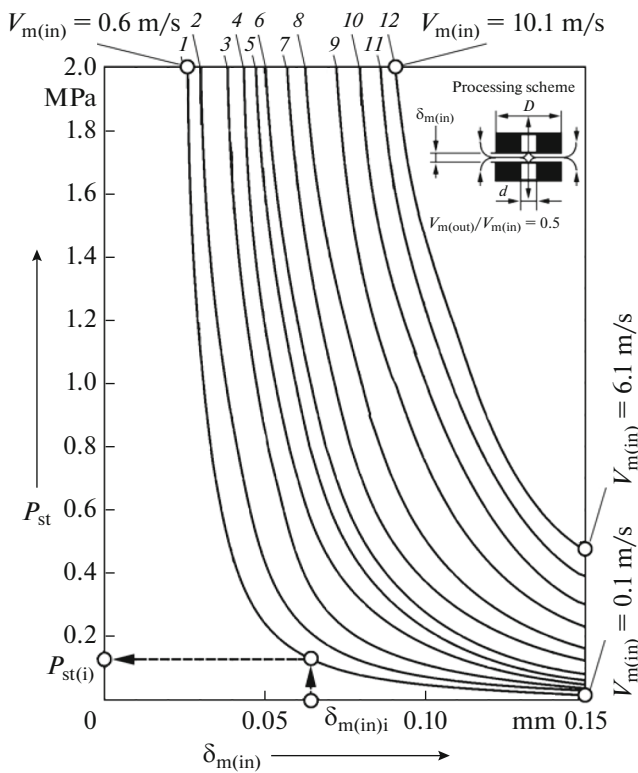


**Fig. 2.** Nomograph to determine static pressure  $P_{st}$  of organic working fluid in tight machine chamber at prescribed values of terminal FSG  $\delta_{t(in)}$  and fluid consumption  $Q$  at DTEA of two plane surfaces (fluid density  $\rho = 875 \text{ kg/m}^3$ , kinematic viscosity  $\nu = 9 \times 10^{-6} \text{ m}^2/\text{s}$ , EW external diameter  $D = 0.17 \text{ m}$ ; hydraulic resistance coefficient at the flow inlet to terminal gap  $\xi_{in} = 0.25$ ; hydraulic resistance coefficient at the flow outlet from terminal gap  $\xi_{out} = 1.8$ ). Key:  $\delta_{t(in)i} \rightarrow Q_i \rightarrow P_{st(i)}$ : (1)  $Q = 0.5 \text{ L/min}$ ; (2)  $Q = 1.0 \text{ L/min}$ ; (3)  $Q = 2.0 \text{ L/min}$ ; (4)  $Q = 3.0 \text{ L/min}$ ; (5)  $Q = 4.0 \text{ L/min}$ ; (6)  $Q = 5.0 \text{ L/min}$ ; (7)  $Q = 7.0 \text{ L/min}$ ; (8)  $Q = 10.0 \text{ L/min}$ ; (9)  $Q = 1.5 \text{ L/min}$ ; (10)  $Q = 2.0 \text{ L/min}$ ; (11)  $Q = 25 \text{ L/min}$ ; (12)  $Q = 30 \text{ L/min}$ .

**RESULTS AND DISCUSSION**

The results of comparative analysis for the received models of the DTEA characteristics of the VK-15 hard alloy in the unipolar (with graphite ET) and bipolar (without ET) modes (see Table 2) that were performed

at  $I = 100 \text{ A}$ ,  $P_{st} = 1.2 \text{ MPa}$ ,  $F = 400 \text{ mm}^2$  are presented in Table 5.

Thus, the performance  $M$  of bipolar DTEA and the specific performance  $M_a$  are considerably greater (by 230%) than the performance and the specific performance of unipolar DTEA. This phenomenon is observed for the first time. Its physical mechanism is associated with the redistribution of energy in the electric arc channel, and it is considered below; the specific consumption of electric energy  $a$  of the bipolar DTEA is lower by a factor of 2.6 than the specific consumption of electric energy by the unipolar DTEA, which positively characterizes the performance of the bipolar DTEA of the plane surfaces of the VK-15 hard alloy samples; the surface roughness  $Ra$  after the bipolar DTEA is 16–27% less than the surface roughness after the unipolar DTEA, which can be explained by the fact that the surface after the unipolar DTEA features only large cathode dimples (Fig. 8a), while the surface after the bipolar DTEA has both large cathode and small anode dimples (Fig. 8b), as the polarity is periodically changed, but no microcracks in the surface layer of the hard alloy sample after DTEA are found (Fig. 9); and a considerable decrease (of 40%) is found in the terminal FSG for the bipolar DTEA in comparison with the unipolar DTEA, as estimated according to the lateral FSG  $\delta_l$  in a certain experiment. As will be shown below, this phenomenon causes the redistribution of energy between the cathode and anode regions and the arc column.

To explain the considerable increase in the process performance at the transition from unipolar DTEA of the hard alloy sample (the electrode pair graphite–VK-15 alloy) to the bipolar DTEA (the electrode pair VK-15 alloy–VK-15 alloy), we present the electric arc as a total of three independent heat sources in the anode and cathode regions and in the arc column:

$$P = P_a + P_c + P_{cl}, \tag{2}$$

where  $P_a$  is the heat power of the anode region of the arc, W;  $P_c$  is the heat power of the cathode region of the arc, W; and  $P_{cl}$  is the heat power of the arc column, W. The source with power  $P_a$ , as is known, situated in

**Table 4.** Mathematical models of physical parameters of arc in bipolar mode of simultaneous DTEA of two VK-15 hard alloy samples

Mathematical model	Scaling relation of factors
Current density in arc $j_s = 550.5 - 25x_1 + 168.5x_2 - 62.5x_3$	$x_1 = 0.02(X_1 - 150)$
Electric field intensity in arc column $E = 638 + 77x_2 - 199x_3$	$x_2 = 5(X_2 - 1)$ $x_3 = 0.00623(X_3 - 560.5)$
Spatial density of heat power in arc column $K = 377 - 35.9x_1 + 148.9x_2 - 151.3x_3$	$x_4 = 4.44(X_4 - 0.275)$

where  $X_1 \rightarrow I, \text{ A}$ ;  $X_2 \rightarrow P_{st}, \text{ MPa}$ ;  $X_3 \rightarrow F, \text{ mm}^2$ ;  $X_4 \rightarrow f, \text{ Hz}$

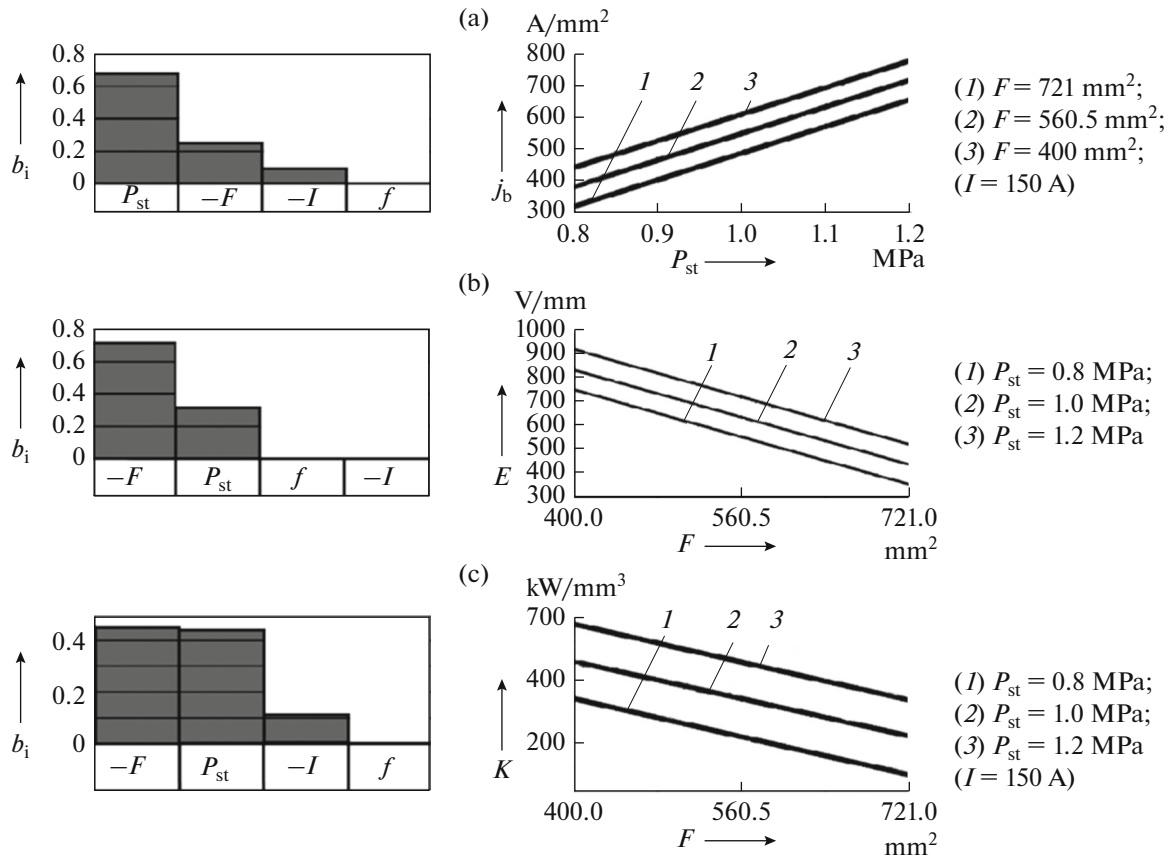


**Fig. 3.** Degree of influence of factors on the physical parameters of the arc in the bipolar mode of simultaneous DTEA of two samples of VK-15 hard alloy: (a) current density in arc  $j_b$ ; (b) electric field intensity in arc column  $E$ ; (c) spatial density of heat power in arc column  $K$ .

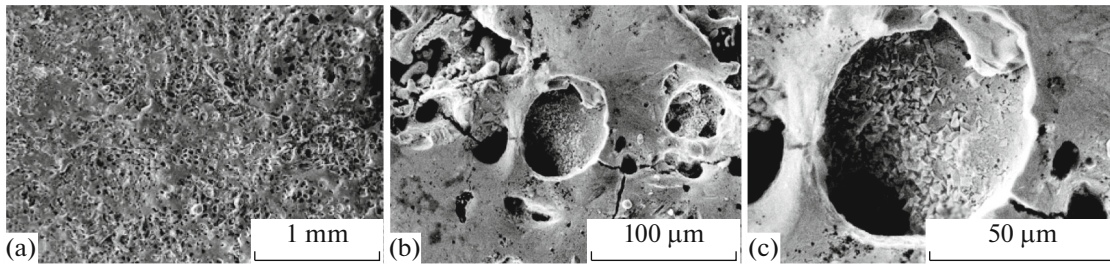


**Fig. 4.** Fractographies of terminal surface of VK-15 hard alloy sample after bipolar DTEA ( $I = 100 \text{ A}$ ;  $P_{st} = 0.8 \text{ MPa}$ ;  $F = 400 \text{ mm}^2$ ): (a)  $\times 40$ ; (b)  $\times 500$ ; (c)  $\times 1200$ .

the plane layer on the anode surface, breaks the anode. The source with power  $P_c$ , situated in the plane layer on the cathode surface, breaks the cathode. Finally, the source with power  $P_{cl}$  situated across the arc column, is responsible for the formation of the arc column length or the terminal FSG.

Within the framework of the comparative analysis of the physical parameters of the electric arc and the process characteristics of the unipolar and bipolar modes of DTEA (Table 3) the experiments were car-

ried out at the same strength of current ( $I = I_{const} = 100 \text{ A}$ ). Thus, if the left-hand and right-hand members of expression (2) are divided by  $I$ , we obtain expression (3), which shows that the heat energies in the anode and cathode regions and in the arc column are in proportion to the voltage falls they experience:

$$U = U_a + U_c + U_{cl}, \quad (3)$$

where  $U$  is the voltage on the arc V;  $U_a$  is the voltage drop in the anode region V;  $U_c$  is the voltage drop in

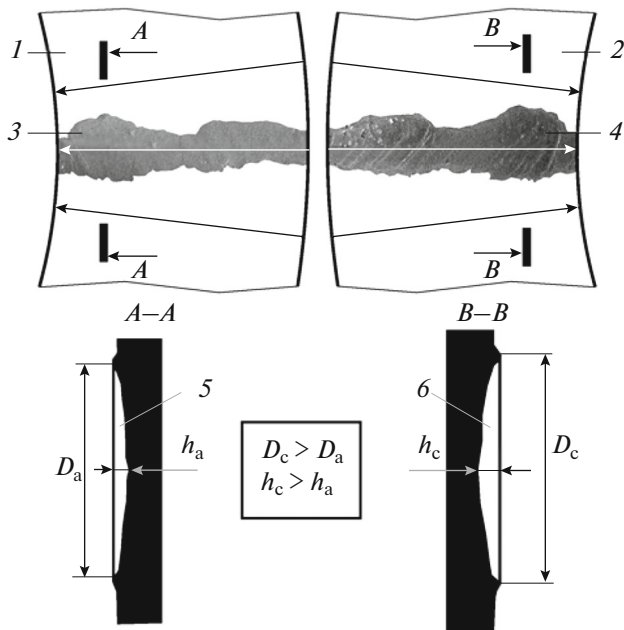
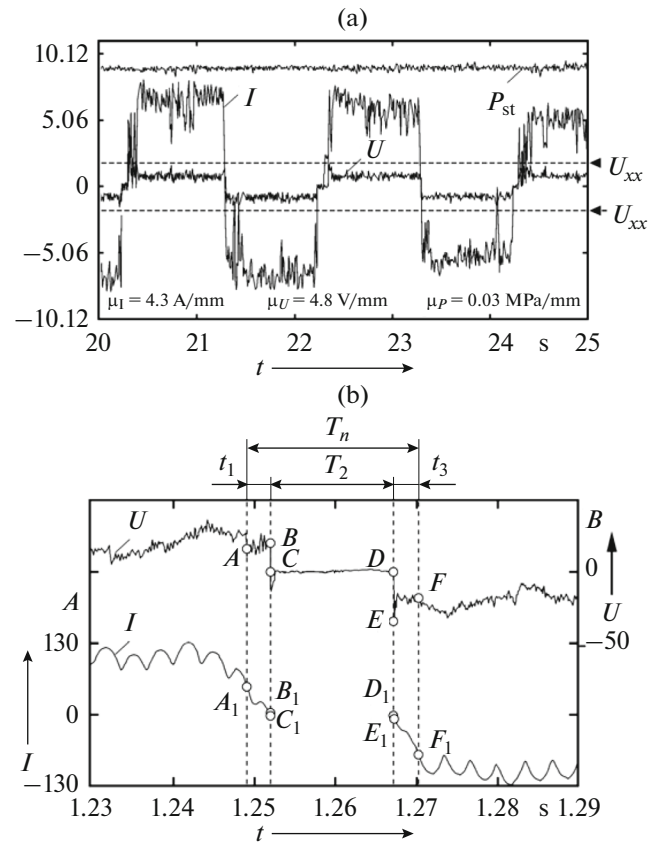


**Fig. 5.** Fractographies of single tracings of arcing in the electrode pair VK-15 alloy–VK-15 alloy”: (1) anode, (2) cathode, (3) fractography of anode tracing, (4) fractography of cathode tracing, (5) profile of anode tracing, (6) profile of cathode tracing.

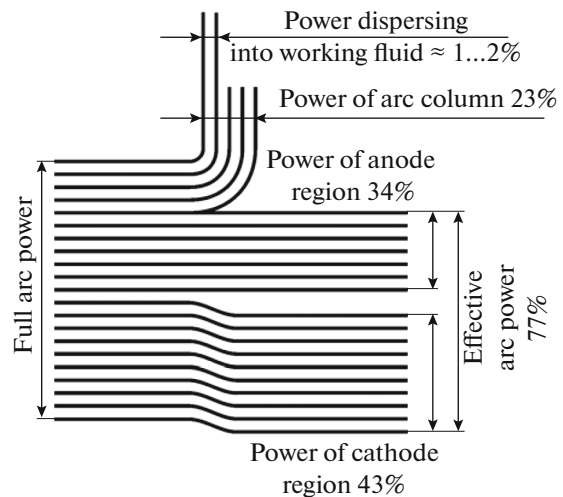
the cathode region  $V$ ; and  $U_{cl}$  is the voltage drop in the arc column  $V$ .

Table 3 shows that at the transition from unipolar DTEA of 45 steel to unipolar DTEA of VK-15 hard alloy, a considerable growth is observed in the total drop in voltages in the anode and cathode regions  $U_{a+c}$  (from 16 V to 19 V), which was determined from the oscillograms with the help of the method of approach between the electrodes. This indicates a growth in the voltage drop in the anode region  $U_a$  and the decrease in the voltage drop in the arc column  $U_{cl}$  (from 14 V to 11 V), and the voltage drop in the cathode region  $U_c$  is the same. In turn, the voltage drop in the arc column leads to a decrease in arc length  $L$  and consequently in the terminal FSG  $\delta$ , which is proven (the gap decreases from 0.10 to 0.05 mm). A similar redistribution of energy is observed between the arc column and the cathode region in favor of the cathode region at the transition from the unipolar DTEA of the VK-15 hard alloy to the bipolar DTEA of two samples of this alloy:  $U_{a+c}$  grows (from 19 to 23 V) as the voltage drop intensifies in the cathode region  $U_c$  due to the decrease in the voltage drop in the arc column  $U_{cl}$  (from 11 to 7 V) as the voltage drop in the anode region  $U_a$  of them is the same; the arc length is reduced, as is shown by the diminution in the terminal FSG (from 0.05 to 0.03 mm).

Thus, in passing from the unipolar DTEA of the hard alloy VK-15 to the bipolar DTEA of two samples



**Fig. 6.** Typical oscillogram (a) and structure of transition process of bipolar DTEA (b) of terminal surface of the electrode pair VK-15 alloy–VK-15 alloy ( $I = 100$  A;  $U = 30$  V;  $P_{st} = 0.8$  MPa;  $F = 400$  mm<sup>2</sup>).



**Fig. 7.** Energy balance of bipolar arc in DTEA conditions.

of this alloy a considerable increase in the heat energy of the cathode region is observed due to the energy of the arc column, which may be greater than the heat energy of the anode region, causing an inversion, i.e.,

**Table 5.** Results of comparative analysis of process characteristics of unipolar and bipolar DTEA of terminal (plane) surfaces of the VK-15 hard alloy samples

Process characteristics	Unipolar DTEA: the pair graphite–VK-15 alloy	Bipolar DTEA: the pair VK-15 alloy–VK-15 alloy
$M$ , mm <sup>3</sup> /min	351	800
$M_a$ , mm <sup>3</sup> /A min	3.51	8
$A$ , kW h/kg	9.99	3.84
$Ra$ , $\mu\text{m}$	$16 \pm 0.5$	$12.5 \pm 0.5$
$\delta_1$ , mm	0.05	0.03
$\gamma$ , %	1.78	–

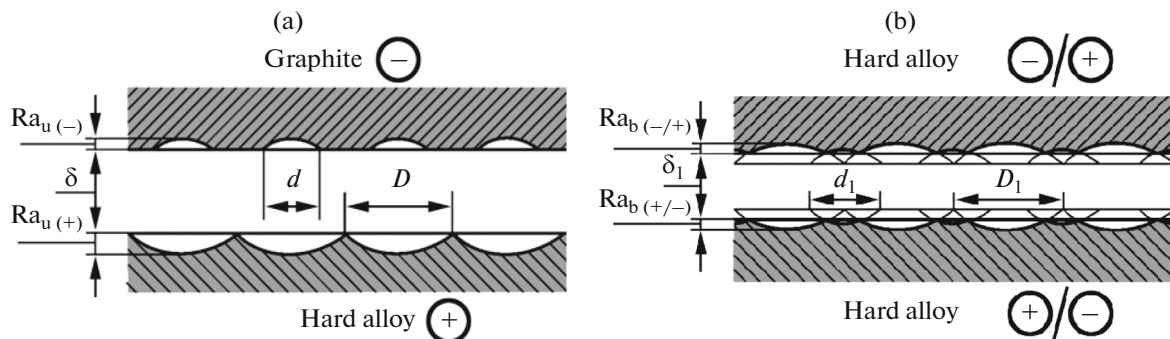
a change in the direction of the dominant electric erosion. This growth in the heat energy of the arc cathode region explains the increase in the performance of the bipolar DTEA of the two samples of the hard alloy VK-15 in comparison with the unipolar DTEA.

The developed analytic dependence (1) for the static pressure of the organic working fluid in the tight machine chamber on a group of factors and the nomograph built on its basis (see Fig. 2) make it possible to determine terminal FSG for the condition of a simultaneous bipolar DTEA of the hard alloy pair (where it is impossible to observe it directly). The terminal FSG, in its turn, allows for the active control of the flow rate and the process characteristics, which mainly relate to the qualities of treatment.

As follows from the analysis of the received mathematical models of the physical parameters of the arc in the bipolar mode of the process of the simultaneous DTEA of the two samples of the hard alloy VK-15 (Table 4, Fig. 3) the average density of the current in the arc  $j_1$  depends on the hydrodynamic factor  $P_{st}$  (a level of influence of 65.8%), with its increases, and on the treatment area  $F$  (24.4%), with its reductions. The intensity of the electric field in arc column  $E$  is mostly influenced by treatment area  $F$  (72.1%), with its reductions, and  $P_{st}$  (27.9%), with reductions in  $E$ . The spatial density of heat power in the arc column  $K$  is fully determined by the treatment area  $F$  (45%) with

the rise in which  $K$  reduces and the static pressure  $P_{st}$  (44.3%), with increases in  $K$ . Under the experimental conditions the electric field intensity in the arc column  $E$  at the bipolar DTEA of the samples of the VK-15 alloy changes from 353 to 1000 V/mm, which is hundreds of times greater than the field intensity in the column of usual welding and plasma arcs. The spatial density of heat power in the arc column  $K$  under the same conditions changed from 99 to 794 kW/mm<sup>3</sup>. The estimation of the spatial density of heat power in the cathode and anode heat sources showed a difference of two orders of magnitude: 29700–674900 kW/mm<sup>3</sup> (cathode region) and 297–6749 kW/mm<sup>3</sup> (anode region).

In the course of bipolar DTEA, using an organic medium, the first arc always has initial contact on the peripheral part of the sample, and the possibility of arcing in the central zone is associated with its agitation by only the erosion products. On this basis, Fig. 10 shows the consequence of arcing in the terminal FSG at the formation of a single dimple, as well as the influence of the erosion products on the DTEA of the whole terminal surface. Thus, there is initially observed the approach of samples 1, 2 (Fig. 10a); then (Fig. 10b), the following occur: an easy contact at place 3; heating, formation of gaseous cavity 4; arc initiation 5, widening the gaseous cavity (Fig. 10c); explosion of the arc; thermal blowout of liquid phase from the dimples into the flow; arcing off; preliminary

**Fig. 8.** Physical mechanism of formation of surface roughness after unipolar (a) and bipolar DTEA (b).

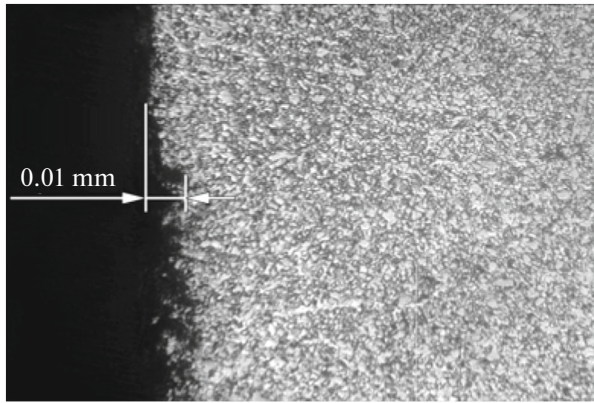


**Fig. 9.** Microstructure of surface layer of VK-15 alloy after DTEA:  $I = 100$  A;  $P_{st} = 1.2$  MPa;  $F = 400$  mm<sup>2</sup>;  $\times 500$ .

formation of a dimple; widening the gaseous cavity to the maximum size; boiling and blowout of an additional portion of metal from the dimples; final formation of a dimple; easy electric contact of rolls at a new place in the direction of the flow with the help of liquid and solid phases 6 of the erosion products; heating; formation of gaseous cavity 7 (Fig. 10d); agitation of the second arc; and possible simultaneous initiation of several arcs (Fig. 10e).

The form of arc tracing is an electroerosion path (see Fig. 5) along the flow of the working fluid in the terminal FSG, i.e., in the direction of the evacuation of the erosion product. The nonuniform tracing width indicates a discrete nature of the break of electrodes: for some time, the arc is in one place, and then it moves to a new place, following the Steenbeck minimum principle. The width and depth of the cathode tracing are greater than the corresponding geometric parameters of the anode tracing. This proves that the heat energy of the arc cathode region is more than the heat energy of the anode region.

The oscillograms of the bipolar DTEA of the terminal surfaces of the electrode pair VK-15 alloy–VK-15 alloy (Fig. 6a) indicate that a peculiarity of the bipolar processing is the existence of a transition process associated with the change in the processing polarity (Fig. 6b). Thus, it appears that the transition process time  $T_1$  does not depend on the processing mode, being determined by the structural features of the contactor transformer. A structural analysis of the transition process time is performed and the duration is determined. In the experiment, the transition process time is 0.021 s. This time does not exceed 0.21% of the polarity cycle. Thus, it is proven that the polarity reversal frequency scarcely influences the process performance of the bipolar DTEA. However, periodic polarity reversal ensures uniform processing of the stock for both electrodes.

For the heat powers of the near-electrode regions and the arc column the efficiency factor of the bipolar

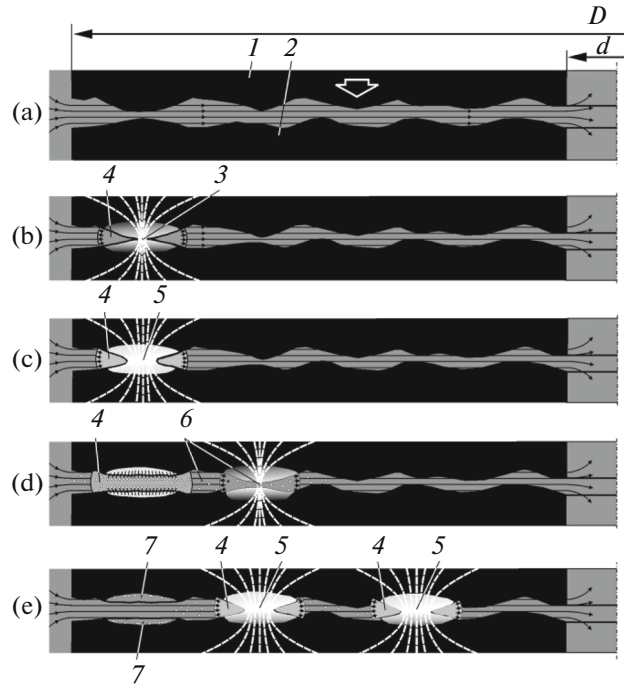


**Fig. 10.** Consequence of arcing in terminal FSG at bipolar DTEA; (1) upper movable hard alloy sample, (2) lower fixed hard alloy sample, (3) contact place, (4) gaseous cavity, (5) electric arc, (6) erosion products, (7) single dimple.

arc is determined in the cross flow of the organic medium for the electrode pair VK-15 alloy–VK-15 alloy. In the experiment, with a current strength of  $I = 100$  A, a working voltage of  $U = 30$  V ( $U_{a+c} = 23$  V,  $U_{cl} = 7$  V),  $P_{st} = 0.8$  MPa,  $f = 0.5$  Hz, and  $F = 400$  mm<sup>2</sup>, the efficiency factor is 77%. Under similar conditions, the efficiency factor of the unipolar arc for the electrode pair graphite ET–VK-15 alloy is lower, by a factor of 2.3, and the economic efficiency of using the bipolar arc for the DTEA of hard alloy parts is 33%.

The bipolar electric arc at DTEA of the hard alloy electrode pair (see Fig. 7) is an effective source of heat, as it efficiently uses electric energy from both anode and cathode regions. For this reason, the performance of the bipolar DTEA increases by 230% in comparison with the unipolar processing of the sample with a graphite ET.

On the basis of the investigations performed, we develop a new method of bipolar high-performance processing of hard-to-cut materials with an electric arc in the hydrodynamic flow of a working fluid with no traditional application of an ET [12].

## CONCLUSIONS

A new method of a high-performance arc processing of two plane surfaces of the parts of hard-to-cut materials in the bipolar mode is proposed, with no traditional application of an electrode tool, which in

comparison with electric arc processing method using an electrode tool ensures an increase in processing performance by 230%.

Mathematical models of the process characteristics of the unipolar DTEA using the graphite ET and bipolar DTEA with no ET are built, which allow the performance, accuracy, and quality of processing to be predicted, as well as a comparison of these two methods of processing and a revelation of the advantages of the bipolar DTEA process.

The physical mechanism of a considerable growth in the DTEA process performance (by 230%) is shown when passing from unipolar (with graphite ET) to bipolar (with no ET) processing is shown to be associated with an inversion that is caused by the redistribution of heat energy between the cathode region and the arc column, in favor of the cathode region.

It is established that arc efficiency at the bipolar DTEA reaches 77%, while arc efficiency for the unipolar DTEA of the electrode pair graphite ET–VK-15 alloy is not more than 33%. This method is a high-performance alternative to traditional methods of processing the hard-to-cut materials.

#### REFERENCES

1. Gorbatyuk, S.M., Shapoval, A.A., Mos'pan, D.V., and Dragobetskii, V.V., *Steel Transl.*, 2016, vol. 46, no. 7, pp. 474–478. doi 10.3103/S096709121607007X
2. Dragobetskii, V.V., Shapoval, A.A., Mospan, D.V., Trotsko, O.V., et al., *Metall. Min. Ind.*, 2015, no. 4, pp. 363–368.
3. Dragobetskii, V.V., Shapoval, A.A., and Zagoryanskii, V.G., *Steel Transl.*, 2015, vol. 45, no. 1, pp. 33–37. doi 10.3103/S0967091215010064
4. Uhlmann, E. and Domingos, D.C., *Proc. CIRP*, 2013, vol. 6, pp. 180–185. doi 10.1016/j.procir.2013.03.10210.1016/j.procir.2013.03.102
5. Demellayer, R. and Richard, J., *Proc. CIRP*, 2013, vol. 6, pp. 89–94. doi 10.1016/j.procir.2013.03.030.10.1016/j.procir.2013.03.030
6. Zolotikh, B.N. and Kruglov, A.I., *Problemy elektroskrovoi obrabotki materialov* (Problems of Electrospark Processing of Materials), Moscow: Tsentr. Nauchno-Issled. Lab. Elektr. Obrab. Mater., 1960, pp. 65–67.
7. Meshcheriakov, G.N., *CIRP Ann.*, 1970, vol. 18, pp. 491–499.
8. Klocke, F., Klink, A., Veselovac, D., Keith, A.D., et al., *CIRP Ann.*, 2014, vol. 63, pp. 703–726.
9. Tamura, T., in *Proc. Seventeenth CIRP Conf. on Electro-Physical and Chemical Machining (ISEM), April 12, 2013*, Leuven, 2013, vol. 6, pp. 117–122.
10. Meshcheriakov, G.N., Nosulenko, V.I., Meshcheriakov, N.G., and Bokov, V.M., *CIRP Ann.*, 1988, vol. 37, no. 1, pp. 209–212.
11. Nosulenko, V.I., *Elektron. Obrab. Mater.*, 2005, no. 1, pp. 8–17.
12. Bokov, V.M., *Rozmirne formoutvorenniya poverkhon' elektrichnoy dugoyu* (Proportional Forming of Surfaces by an Electric Arc), Kirovograd: Imeks-LTD, 2002.
13. Bokov, V.M. and Sisa, O.F., UA Patent 45498, *Byull. Izobret.*, 2009, no. 21.

Translated by M. Myshkina